Multiphasic Nanostructured Composite: Multi-Dye Tunable Solid State Laser

Gary Ruland, Raz Gvishi, and Paras N. Prasad*

Contribution from the Photonics Research Laboratory, Department of Chemistry, State University of New York at Buffalo, Buffalo, New York 14260-3000

Received August 24, 1995[⊗]

Abstract: In this paper we present a new concept to control the energy transfer between two components using novel multiphasic nanostructured composites. The example studied here consists of two lasing dyes (Rhodamine-6G and *trans*-4-[*p*-(*N*-ethyl-*N*-(hydroxyethyl)amino)phenylstyryl]-*N*-(hydroxyethyl)pyridinium iodide (ASPI)), each of which resides in two different phases of a multiphasic composite. The energy transfer between these two phases was studied and found to be insignificant. Therefore, this composite exhibited lasing from both dyes. The multiphasic matrix was tunable through the range of both dyes from 560 to 610 nm with an efficiency of ∼7%. The lasing properties of this lasing media were studied compared to reference dye solutions. In the solution state a mixture dye solution exhibited complete quenching of one of the dyes (Rhodamine-6G). The quenching mechanism in the solution state and its lack in the solid state matrix is proposed. In addition, the new laser dye, ASPI, has been characterized by its linear spectroscopy and lasing properties in solution. The results of this characterization reveal a dye with a low fluorescence quantum yield ($\sim 7 \times 10^{-3}$), but high lasing efficiency (∼13.5%) under pulsed pumping conditions. An intersystem crossing from the S_1 to T_1 state may be responsible for this phenomenon.

Introduction

To develop optics and photonics to their largest potential is a goal of all researchers in the field of lasers and nonlinear optics. To accomplish this goal, multifunctional materials need to be developed which simultaneously satisfy many functional requirements and at the same time possess high optical quality.[1,2] Single multifunctional devices have the potential to perform the tasks of many different devices. In addition, if the system is chosen carefully, it may also be possible to enhance a specific effect in the device. We believe that multiphasic nanostructured composite glass is a new class of optical materials that have tremendous opportunities to enhance the development of the field of photonics.

Progress in the last decade in the design of organic systems has led to the development of promising materials that possess lasing and nonlinear optical properties.[3,4] More recently a major effort has been centered on photostable host matrices into which optically active organic species can be introduced. Examples of such matrices are the sol-gel derived matrices: silica-gels,[5−9] alumina-gels,[10,11] ormosils,[12] composite films,[13] and composite glasses.[14−16] We recently reported optical power limiting behavior from two distinct phases in a multiphasic nanostructured composite, thereby operating over a wide wavelength range covering both components.[17,18] Each of the species has different power limiting mechanisms at different wavelengths and no interaction between the two dopants could be detected.

By controlling the phase separation on a nanometer size scale, the structure and dynamics in the nanostructured composites can be controlled to produce multifunctional bulk forms of excellent optical quality. In this paper, we illustrate this concept by using a multiphasic composite containing two different lasing dyes which reside in different phases and have an insignificant energy transfer between the phases. Thus, the quenching mechanism which exists in a single phase can be reduced using a multiphasic composite. The result is that lasing can be observed from both dyes yielding a broad tunability range for lasing.

One of the most important applications of dye-doped solid matrices is the solid-state dye laser which allows one to achieve tunability in a solid state device.[19] Until recently liquid dye lasers were the main system used to achieve tunability in the visible. However, solid state dye lasers have advantages over liquid dye lasers by being nonvolatile, nonflammable, nontoxic,

* Author to whom all correspondence should be sent.

[⊗] Abstract published in *Advance ACS Abstracts,* March 1, 1996.

(1) Prasad, P. N.; Williams, D. J. *Introduction to Nonlinear Optical Effects in Molecules and Polymers*; Wiley: New York, 1991.

(2) Bruzynski, R.; Prasad, P. N. *Photonics and Nonlinear Optics with Sol-Gel Processed Inorganic Glass: Organic Polymer Composite*; Klein, L. C., Ed.; Kluwer Academic: Boston, 1994; Chapter 19.

(3) Prasad, P. N.; Rhinhardt, B. A. *Chem. Mater*. **1990**, *2*, 660.

(4) Burland, D. M.; Miler, R. D.; Walsh, C. A. *Chem. Rev*. **1993**.

(5) Altshuler, G. B.; Bakhanov, V. A.; Dulneva, E. G.; Erofeev, A. V.; Mazurine, O. V.; Roshova, G. P.; Tsekhomskaya, T. S. *Opt. Spectrosc*. **1987**, *62*, 709.

(6) Whitehurst, C.; Shaw, D. J.; King, T. A. *SPIE Proc*. **1990**, *1328*, 183.

(7) Mckiernan, J. M.; Yamanaka, S. A.; Knobbe, E. T.; Pouxviel, J. C.; Parveneh, S.; Dunn, B.; Zink, J. I. *J. Inorg. Organomet. Polym*. **1991**, *164*, 87.

(8) Gvishi, R.; Reisfeld, R. *J. Non-Crystl. Solids* **1991**, *128*, 69.

(9) Salin, F.; Le Saux, G.; Georges, P.; Brun, A.; Bagnall, C.; Zarzycki, J. *Opt. Lett*. **1989**, *14*, 785.

(10) Kobayashi, Y.; Kurokawa, Y.; Imai, Y.; Muto, S. *J. Non-Cryst. Solids* **1988**, *105*, 198.

(11) Mckiernan, J. M.; Yamanaka, S. A.; Dunn, B.; Zink, J. I. *J. Phys. Chem*. **1990**, *94*, 5652.

(12) Knobbe, E. T.; Dunn, B.; Fuqua, P. D.; Nishida, F. *Appl. Opt*. **1990**, *29*, 2729.

(13) Bruzynski, R.; Prasad, P. N. Photonics and Nonlinear Optics with Sol-Gel Processed Inorganic Glass: Organic Polymer Composite. *Sol-Gel Optics: Processing and Applications*; Klein, L., Ed.; Kluwer Academic Publishers: Dordrecht, The Netherlands, 1993; Chapter 19.

(14) Pope, E. J.; Asami, M.; Mackenzie, J. D. *J. Mater. Res*. **1987**, *29*, 1.

(15) Gvishi, R.; He, G. S.; Prasad, P. N.; Narang, U.; Li, M.; Bright, F. V.; Reinhardt, B. A.; Dillard, A. G. *Appl. Spectrosc*. **1995**, *49*, 82.

(16) Gvishi, R.; Narang, U.; Prasad, P. N.; Bright, F. V. *Chem. Mater*. In press.

(17) Gvishi, R.; Bhawalkar, J.; Kumar, D. N.; Ruland, G.; Narang, U.; Prasad, P. N. *Chem. Mater*. Submitted for publication.

(18) Prasad, P. N.; Gvishi, R.; Ruland, G.; Kumar, D. N.; Bhawalkar, J.; Narang, U. *SPIE Proc*. In press.

(19) Durate, F. J. *Laser Focus World* **1995**, May, 187.

0002-7863/96/1518-2985$12.00/0 © 1996 American Chemical Society

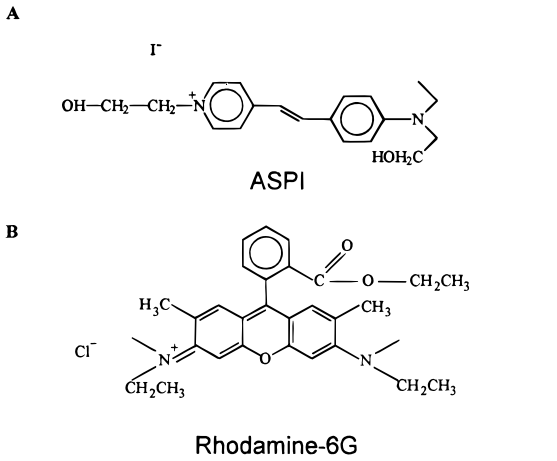

Figure 1. Molecular structures of *trans*-4-[*p*-(*N*-ethyl-*N*-(hydroxyethyl)amino)phenylstyryl]-*N*-(hydroxyethyl)pyridinium iodide (ASPI) and Rhodamine-6G.

compact, and mechanically stable. The problem of heat dissipation, however, poses a serious impediment for their utilization in applications that require high powers under either cw or pulsed high repetition rate operation. In liquid dyes, on the other hand, a flowing solution or a jet is a practical means of solving the heat problem. In both cases photostability is a property of prime importance for selecting a laser dye.[20]

In recent years lasing from dye-doped solid matrices was demonstrated by several groups via a one-photon excitation process[21−27] and even via a two-photon excitation process.[28,29] As was addressed previously, the advantage of a solid state dye laser depends heavily on its photostability and mechanical properties. From the matrices which have been previously studied, sol-gel derived composite glass is a promising matrix due to its high photostability,[30] optical quality, and mechanical stability compared to the other discussed matrices.[17,31,32]

In this paper we present the results of a novel multiphase nanocomposite glass monolith containing two laser dyes, *trans*-4-[*p*-(*N*-ethyl-*N*-(hydroxyethyl)amino)phenylstyryl]-*N*-(hydroxyethyl)pyridinium iodide (ASPI)[29] and Rhodamine-6G, in which the energy transfer between the two components is minimized to produce tunable laser output across the lasing region of both ASPI and Rhodamine-6G. The molecular structures of ASPI and Rhodamine-6G are given in Figure 1. We present the basic spectroscopic properties of the new laser dye, ASPI in ethanol solution, and a mixed solution of ASPI and Rhodamine-6G in ethanol. We propose the mechanism for quenching in the solution state and the lack of it in the composite glasses. Rhodamine-6G was chosen because of its very high lasing efficiency and solubility properties. Furthermore, this lasing dye has been extensively studied. One of the major drawbacks of Rhodamine-6G is its lack of photostability.[30,33] ASPI was chosen for its solubility characteristics, spectroscopic features, and lasing properties.[29] A related compound ASPT (which differs in the nature of the counterion) has exhibited very efficient two-photon pumped up conversion lasing when pumped at 1064 nm from a pulsed Q-switched Nd:YAG laser.[28] ASPI's linear spectroscopic features and lasing properties in solution are characterized in this paper in addition to those in the composite glass.

Experimental Section

Composite Preparation. The procedure used to prepare highly porous silica-gel bulk glasses was described previously by Gvishi et al.[15,16] The sol-gel was prepared from a precursor solution of tetraethylorthosilicate (TEOS) (Aldrich 99+% pure) and ethanol at a molar ratio of 1:4. After 1 h, water (molar ratio 4) and HNO_3 (Aldrich A.C.S. reagent, molar ratio 0.06) were added. This step was followed by the addition of HF (Aldrich 48 wt% in water, 99.99+% pure, molar ratio 0.8). After mixing, the solution was placed in a 4.5-mL polystyrene cuvette and covered with parafilm containing three pin holes in the top. The cuvettes were then placed in an oven (Precision Scientific Freas Mechanical Convection Oven, Model 605), set at 45 °C, for 2 weeks. The bulk gels were then removed and placed in a furnace (Fisher Scientific Isotemp Programmable Furnace, Model 495A) for drying and partial densification to glass by slow heating (50 °C/h) from room temperature to 500 °C. The dimensions of the final glass are approximately 10 mm × 5 mm × 5 mm. Sol-gel glasses prepared by this method have the following characteristics: average pore diameter of 46 Å, specific surface area of ∼850 m^2/g, and a pore volume of 68%.[16,31]

Three separate glasses were then prepared, one containing ASPI (which was synthesized in our lab,[29] see Figure 1 for its molecular structure), one containing Rhodamine-6G (Aldrich 99% pure), and one containing both dyes. The ASPI glass was prepared by placing the porous glass in a solution of ASPI in ethanol (4.4×10^{-3} M). After the solution completely impregnated the glass it was removed from the solution and placed on a hot plate at ∼45 °C for several hours until the ethanol evaporated out of the glass leaving behind ASPI on the surface of the pores. This procedure resulted in a concentration of $\sim 3.1 \times 10^{-3}$ M (this concentration represents the volume of the pores of the glass, ∼70%, and assumes that all of the chromophores deposited on the walls of the pores). The glass was then immersed in a methyl methacrylate (MMA, Aldrich 99% pure) monomer containing 2 wt % of 2,2′-azobis(isobutyronitrile) (AIBN, Polysciences, Inc.), a thermal polymerization initiator, for insitu polymerization. After the glass was completely impregnated with MMA (∼30 min) it was removed and placed in a vial containing MMA and AIBN (0.5 wt %). The vial was closed and placed in the Freas oven at 45 °C for full polymerization (several days).

The Rhodamine-6G composite glass was prepared by dissolving Rhodamine-6G in MMA. A surfactant (Triton X-100 Aldrich) was added to minimize any aggregation. The concentration of the Rhodamine-6G/MMA solution was $\sim 1 \times 10^{-4}$ M. The solution was then split; into one portion 2 wt % AIBN was added and into the other portion 0.5 wt % AIBN was added. A porous glass was immersed into the 2% AIBN/MMA solution until completely impregnated and then transferred to the 0.5 wt % AIBN/MMA solution in a vial. The vial was capped and allowed to fully polymerize in the same fashion as the ASPI doped glass. The final concentration of Rhodamine-6G in the composite glass is approximately 6.5×10^{-5} M (corresponding to the porosity of the glass).

The glass containing both dyes (duel composite) was prepared exactly (same concentrations and processes) as described above by doping the

(20) Cunningham, R. *Laser Optronics* **1991**, Feb 30.
(21) Reisfeld, R.; Brusilovsky, D.; Eyal, M.; Miron, E.; Burshtein, Z.; Ivri, J. *SPIE Proc.* **1989**, *1182*, 230.
(22) Gvishi, R.; Reisfeld, R.; Miron, E.; Burshtein, Z. *SPIE Proc.* **1993**, *1972*, 390.
(23) Shamrakov, D.; Reisfeld, R. *Chem. Phys. Lett.* **1993**, *213*, 47.
(24) He, G. S.; Zhao, C. F.; Park, C. K.; Prasad, P. N.; Burzynski, R. *Opt. Commun.* **1994**, *111*, 82.
(25) Dunn, B.; Zink, J. I. Sol-gel Encapsulated Molecules: Optical Probes and Optical Properties. *Sol-Gel Optics: Processing and Applications*; Klein, L., Ed.; Kluwer Academic Publishers: Dordrecht, The Netherlands, 1993; Chapter 14.
(26) Lo, D.; Parris, J. E.; Lawless, J. C. *Appl. Phys. B.* **1993**, *56*, 385.
(27) Canva, M.; Dubois, A.; Georges, P.; Brun, A. *SPIE Proc.* **1994**, *2288*, 298.
(28) He, G. S.; Bhawalkar, J. D.; Zhao, C. F.; Prasad, P. N. *IEEE J. Quant. Electron.* Submitted for publication.
(29) Zhao, C. F.; He, G. S.; Bhawalkar, J. D.; Park, C. K.; Prasad, P. N. *Chem. Mater.* In press.
(30) Gvishi, R.; Reisfeld, R.; Burshtein, Z. *J. Sol-Gel Sci. Tech.* **1995**, *4*, 49.
(31) Gvishi, R. Ph.D. Thesis, The Hebrew University of Jerusalem, Jerusalem, Israel, 1993.
(32) Klein, L. Nanocomposite Fabrication for Transparent Windows. *Sol-Gel Optics: Processing and Applications*; Klein, L.; Kluwer Academic Publishers: Dordrecht, The Netherlands, 1993; Chapter 10.
(33) Antonov, V. S.; Hola, K. L. *Appl. Phys. B* **1983**, *32*, 9.

Table 1. Spectroscopic and Lasing Parameters for ASPI and Rhodamine-6G in Solution and in Composite Glass

	solution state			composite glass		
	ASPI	Rhodamine-6G	ASPI/Rhodamine-6G	ASPI	Rhodamine-6G	ASPI/Rhodamine-6G
absorbance maximum	483 nm	530 nm				
molar absorbtivity	6.8×10^{-4}	1.05×10^{-5}				
fluorescence maximum	600 nm	562 nm	595 nm		546 nm	594 nm/552 nm
fluorescence fwhm	38 nm	25 nm	40 nm	45 nm	53 nm	41 nm/43 nm
stokes shift	118 nm	32 nm				
quantum yield	6.5×10^{-3}	0.9				
lasing characteristics						
efficiency	13.5%	25.2%		9.4%	3.8%	7.3%
tunability range (fwhm)	599−635 nm	562−584 nm	598−643 nm	585−606 nm	561−573 nm	564−601 nm

ASPI first, followed by the Rhodamine-6G/MMA and subsequent in-situ polymerization as described above. The ASPI composite glass has ASPI which is adsorbed onto the walls of the pores (interfacial phase); the Rhodamine-6G composite glass has Rhodamine-6G in the polymer phase (PMMA). The duel composite glass has ASPI in the interfacial phase while Rhodamine-6G resides in the polymer phase. The duel composite glass is, therefore, called a multiphasic nanostructured composite glass.

After the polymerization was complete, the glasses were removed from the surrounding poly(methyl methacrylate) (PMMA) by a chloroform wash. The glasses were then polished (Buehler Metaserv 200 grinder−polisher) in seven incremental steps, starting with a 180 grit up to a 4000 grit SiC paper and going down from a 1 μm to a 0.25 μm diamond paste.

Optical Measurements. The absorption spectra were obtained using a Shimadzu UV−vis 260 spectrophotometer with a resolution of ±1 nm. The solution state spectra were obtained using quartz cuvettes (1 cm path length) throughout.

The emission spectra were collected on a Shimadzu RF-5000U spectrofluorophotometer (90° geometry). For solution state measurements a fluorometric quartz cuvette was used. For the composite glass, the emission was obtained from the surface of the glass (90° geometry) due to significant primary absorption. The resolution of the spectrofluorometer is ±2 nm.

The system used in our lasing performance studies (both the solution and the composite glass) was a frequency-doubled Quanta-Ray DCR Nd:YAG Q-switched laser with a repetition rate up to 30 Hz producing 8 ns pulses at 532 nm. During all of the lasing experiments the outcoming beam was reflected using a second harmonic selector and passed through an IR filter. The beam was then passed through an aperture, followed by a cylindrical lens to focus the beam to a linear shape on the sample, which was in a transverse pump cavity configuration. The cavity consisted of a ∼100% reflecting flat mirror (at 0°) and a ∼70% reflecting flat outcoupler (at 0°) through the range of 550 to 630 nm.

For the lasing slope efficiency measurements in solution all measurements were carried out at a repetition rate of 30 Hz. The pump beam and the lasing output were measured with a Scientech 362 power-energy meter. The lasing efficiency measurements in composite glasses were carried out at a repetition rate of 1 Hz. The pump beam and the lasing output were measured with a United Detector Technology 350 linear/log optometer; each collected data point was an average of 10 pulses. The lasing efficiencies were calculated from the slope without any additional corrections.

The lasing output vs wavelength of the composite glasses was measured by passing the lasing output through a monochromator (SPEX Triplemate Model 1460) and collected on an optical multichannel analyzer (OMA-III, EG&G Princeton Applied Research). The spectrum is a collection of 11 pulses at a 1 Hz repetition rate.

The tunability measurements were carried out at a repetition rate of 1 Hz on the composite glasses and 2 Hz in the solution state. The ∼100% reflecting mirror was replaced with a 1200 groove/mm grating, and the lasing output was collected through a monochromator (Jobin-Yvon UV monochromator) with a resolution of ±1.6 nm and focused onto a fast photodiode (Si PIN). The output lasing intensity was attenuated by neutral density filters (ESCO Products Inc.) to avoid saturation of the photodiode. The output signal was measured with an oscilloscope (Tektronix 350 MHz, Model 2467). The wavelength was scanned manually, each data point was an average of 10 pulses, and several measurements were made to ensure repeatability.

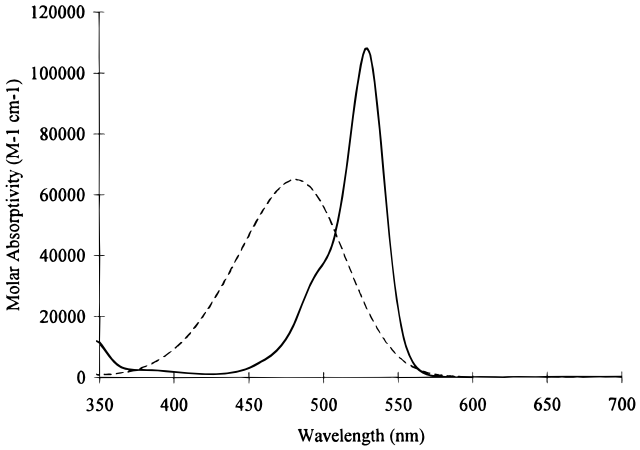

Figure 2. Molar absorptivity as a function of wavelength in ethanol solution: the dashed curve is for ASPI and the solid curve is for Rhodamine-6G.

Results and Discussion

Optical Characterization of the Solution State. The molar absorptivity of ASPI in ethanol was determined by measuring five solutions ranging from $2.6 \times 10^{-}16$ to 2.5×10^{-5} M. A plot of absorption at the maxima (483 nm) vs concentration yielded a straight line and by Beer's law the slope yielded a molar absorptivity of 6.8×10^4 M^{-1} cm^{-1}. The molar absorptivity of Rhodamine-6G is well-known (1.05×10^5 M^{-1} cm^{-1} at 530 nm) in ethanol.[34] From these values a plot of the absorptivity as a function of wavelength was generated and is shown in Figure 2. The absorption maximum of ASPI is 483 nm and that of Rhodamine-6G is 530 nm. Both ASPI and Rhodamine-6G have the same extinction coefficient at 509 nm. The observed data are summarized in Table 1.

The fluorescence emission spectra of ASPI (3.1×10^{-3} M), Rhodamine-6G (6.5×10^{-5} M), and a mixed solution of ASPI (3.1×10^{-3} M) and Rhodamine-6G (6.5×10^{-5} M) in ethanol are shown in Figure 3. These concentrations were chosen to be comparable with the concentrations in the final composite glass. The concentrations used are 70% of the concentration of the solutions used to dope the glasses, which corresponds approximately to the porosity of the glass. The excitation used is 509 nm since the dyes have the same molar absorptivity at this wavelength. The emission maxima for Rhodamine-6G, ASPI, and the mixture solution are 562, 600, and 595 nm, respectively. The approximate width of the emission, full width at half maximum (fwhm), is 25 nm for Rhodamine-6G, 38 nm for ASPI, and 40 nm for the mixed solution. Rhodamine-6G

(34) *Lambdachrome Laser Dyes Data Sheet*; Brackmann, U., Ed.; Lambda Physik: Göttingen, 1994; p 151.

(35) Reisfeld, R. *Natl. Bur. Stand.* **1972**, *76A*, 613.

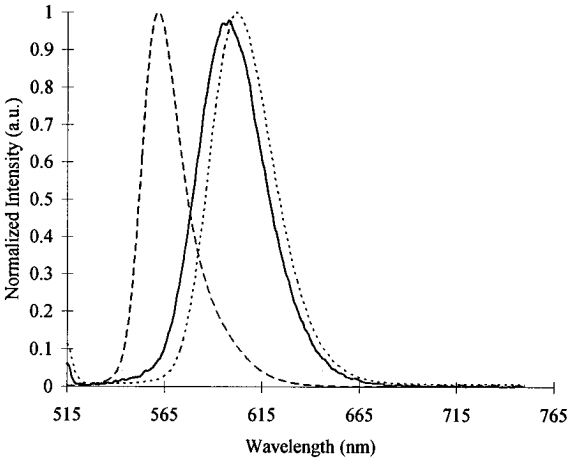

Figure 3. Fluorescence emission of Rhodamine-6G (6.5×10^{-5} M; dashed curve), ASPI (3.1×10^{-3} M; dotted curve), and a mixed solution containing Rhodamine-6G and ASPI (6.5×10^{-5} M/3.1×10^{-3} M, respectively; solid curve). The solvent for each solution was ethanol.

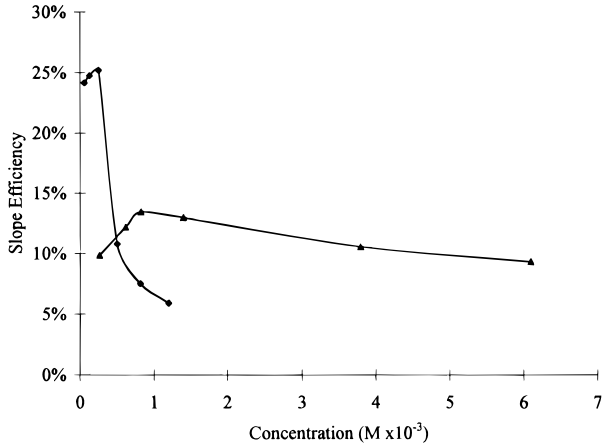

Figure 4. Lasing slope efficiency as a function of concentration in ethanol solution. ASPI is represented by triangles, and Rhodamine-6G is represented by diamonds. The dyes were transverse pumped with a 8 ns pulsed frequency-doubled Nd:YAG laser at 532 nm operating at a 30 Hz repetition rate.

has a Stokes shift of 32 nm and exhibits an asymmetric peak that can be attributed to self absorption at this concentration. ASPI has a very large Stokes shift of 118 nm and the self-absorption process is insignificant for this dye. Large Stokes shifts were previously attributed to a different charge distribution in the excited state compared to the ground state as it was reported for Coumarin dyes.[36] It is also evident from the emission spectra that emission from Rhodamine-6G is completely quenched in the mixture when combined with ASPI in such concentrations.

The fluorescence quantum yield was obtained by measuring the emission of Rhodamine-6G and ASPI in separate solutions. A comparative method was used according to the following equation.[35]

$$\Phi_s = \Phi_r \frac{n_s A_r \int F_s}{n_r A_s \int F_r} \quad (1)$$

Here Φ_s is the quantum yield of the sample, Φ_r is the quantum yield of the reference, n_s is the refractive index of the sample, n_r is the refractive index of the reference, A_s is the absorbance of the sample at the pump wavelength, A_r is the absorbance of the reference at the pump wavelength, $\int F_s$ is the integral of the fluorescence emission of the sample (in cm^{-1} units), and $\int F_r$ is the integral of the fluorescence emission of the reference (in cm^{-1} units). The fluorescence quantum yield of Rhodamine-6G used was taken as 0.95.[36] The emission of both dyes was measured when excited at 509 nm where the concentrations of the dyes are the same (2.6×10^{-6} M). This produced a fluorscence quantum yield for ASPI of 7×10^{-3}. A second measurement was carried out where ASPI was at a concentration of 1.8×10^{-6} M and Rhodamine-6G was at a concentration of 2.6×10^{-6} M. ASPI was excited at 482 nm and Rhodamine-6G was excited at 509 nm. At these two wavelengths both dyes have the same molar absorptivity at their respective concentrations. This measurement produced a fluorescence quantum yield for ASPI of 6×10^{-3}. ASPI, therefore, has a fluorescence quantum yield that is two orders of magnitude lower than that of Rhodamine-6G. The observed fluorescence quantum yield is presented as well in Table 1.

Figure 4 shows the lasing slope efficiency of both Rhodamine-6G and ASPI in ethanol as a function of concentration. Rhodamine-6G was observed to be most efficient at a concentration of 2.5×10^{-4} M with a lasing slope efficient of 25.2% under the conditions of our experiment. The optimized Rhodamine-6G concentration observed is the same as that recommended by literature but with a higher efficiency than we observed.[34] It may be a consequence of using a simple cavity in the present case. ASPI was found to be most efficient at a concentration of 8.2×10^{-4} M with a lasing slope efficiency of 13.5%. The difference between the lasing slope efficiency behavior of Rhodamine-6G and that of ASPI is significant noting a sharp drop off of efficiency in Rhodamine-6G due to self-absorption and the lack of it in ASPI. The measurement of the lasing efficiency of ASPI was terminated at a concentration of 6.1×10^{-3} M which is the limit of solubility of ASPI in ethanol. The observed data are also summarized in Table 1.

The relatively high lasing slope efficiency of ASPI is surprising considering the low fluorescence quantum yield of ASPI relative to Rhodamine-6G. This result may indicate that the low quantum yield of ASPI is caused by a radiationless energy loss that occurs on the time scale of the excited state lifetime under continuous pumping conditions. We believe that in the cavity, with the short pulsed pumping used, the dye is stimulated to emit a photon at a much faster rate than the nonradiative processes. This phenomenon is well-known[37] and has been demonstrated using dyes that have fluorescence quantum yields as low as 5×10^{-4} with lasing conversion efficiencies of 10 to 20%.[38] In our case, it is likely that there is an intersystem crossing occurring from the S_1 state to the T_1 state.[37] This implies that the dye would not be suitable for cw lasing and it could possibly act as a saturable absorber (or a reverse saturable absorber). It also implies that ASPI's quantum yield and lasing properties are related to the pumping rise time.[37] It is also interesting that this chromophore (with a different counterion, tetraphenylborate), as mentioned earlier, can operate as a two-photon excitation induced laser when pumped at 1064 nm.[28] Although iodide is a well-known quenching ion[36] we did not observe any difference in the spectroscopic and lasing performance between the two derivatives. It is likely many dyes which have not been considered for lasing, due to their low fluorescence quantum yield, may be very effective laser dyes under pulsed pumping conditions and may also exhibit a strong

(36) Drexhage, K. H. Structure and Properties of Laser Dyes. *Dye Lasers*; Schäfer, F. P., Ed.; Springer-Verlag: Berlin, 1990; Chapter 5.

(37) Schäfer, F. P. Principles of Dye Laser Operation. *Dye Lasers*; Schäfer, F. P., Ed.; Springer-Verlag: Berlin, 1990; Chapter 1.

(38) Polland, H. J.; Elsaesser, T.; Seilmeier, A.; Kaiser, W. *Appl. Phys. B* **1983**, *32*, 53.

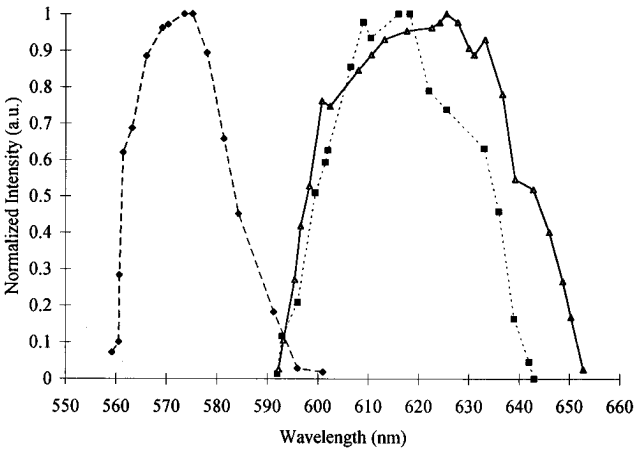

Figure 5. Lasing tunability of Rhodamine-6G (6.5×10^{-5} M), ASPI (3.1×10^{-3} M), and a mixture containing Rhodamine-6G and ASPI (6.5×10^{-5} M/3.1×10^{-3} M, respectively). Rhodamine-6G is represented by diamonds, ASPI by squares, and the mixed solution by triangles. The dyes were transverse pumped with a 8 ns pulsed frequency-doubled Nd:YAG laser at 532 nm operating at a 2 Hz repetition rate, using a grating as the back reflector.

two-photon absorption cross section. By chemically modifying ASPI through the introduction of a bridging group the quantum yield might be enhanced (as has been demonstrated for Rhodamines).[36]

The lasing tunability of ASPI (3.1×10^{-3} M), Rhodamine-6G (6.5×10^{-5} M), and a mixture of ASPI (3.1×10^{-3} M) and Rhodamine-6G (6.5×10^{-5} M) in ethanol is shown in Figure 5. The observed fwhm are as follows: 37 nm for ASPI, 22 nm for Rhodamine-6G, and 45 nm for the mixed solution. The tunability wavelength range is presented in Table 1. It is also apparent that there is no contribution from Rhodamine-6G in the mixture. However, there is a significant increase in the range of the tunability of the mixture which is evident of a higher lasing efficiency probably due to an effective energy transfer from Rhodamine-6G to ASPI. We believe that the energy transfer is accomplished through a Förster mechanism which results in fluorescence quenching of Rhodamine-6G in the mixture. Another possible quenching mechanism is dynamic quenching, which is given by:[39]

$$\frac{\Phi_f}{\Phi_f^0} = \frac{1}{1 + K_q[Q]} \tag{2}$$

where Φ_f^0 is the fluorescence quantum yield in the absence of quenching, and Φ_f is the fluorescence quantum yield in the presence of the quencher. K_q in eq 2 is the Stern−Volmer constant defined as $K_q = k_q\tau_f^0$, where k_q is the dynamic quenching rate; τ_f^0 is the fluorescence lifetime in the absence of the quencher. [Q] is the concentration of the quencher.

In aqueous solution at room temperature, the bimolecular collision rate is about 10^{10} L mol^{-1} s^{-1}.[40] If all collisional encounters result in quenching we can estimate the maximum value of k_q to be about 10^{10} L mol^{-1} s^{-1}. In our case the fluorescence lifetime of Rhodamine-6G is ∼3.9 ns[41] and the quencher concentration is 3.1×10^{-3} M which yields a maximum quenching of only ∼10%. Therefore, we do not consider dynamic quenching to be the dominate mechanism for the quenching of Rhodamine-6G. The most probable quenching mechanism is Förster energy transfer which is inversely related to the sixth power of the distance between the donor and the acceptor.[42] A simple calculation of the distance between the centers of two molecules was done using the following equation:

$$d = 3\sqrt{\frac{1000}{CN_a}} \tag{3}$$

where d is the distance between the molecules in cm, C is the concentration in mol/L, and N_a is Avogadro's number. This calculation reveals that the distance between the dye molecules, evenly distributed in the mixture solution, is 80 Å for ASPI to ASPI and 295 Å for Rhodamine-6G to Rhodamine-6G. When determining the distance between the Rhodamine-6G and the ASPI molecules, Rhodamine-6G was placed at the center of a cube, with ASPI at the corners of the cube, at a distance of 80 Å, and the calculation indicates a distance of 70 Å for ASPI to Rhodamine-6G. The distance between the ASPI and Rhodamine-6G molecules is well within the range where Förster energy transfer can occur.[42] Additional discussion is presented later in this paper regarding the Förster energy transfer mechanism in the composite glass case compared to the solution state. A more systematic study of the quenching process in solution will be conducted in the future.

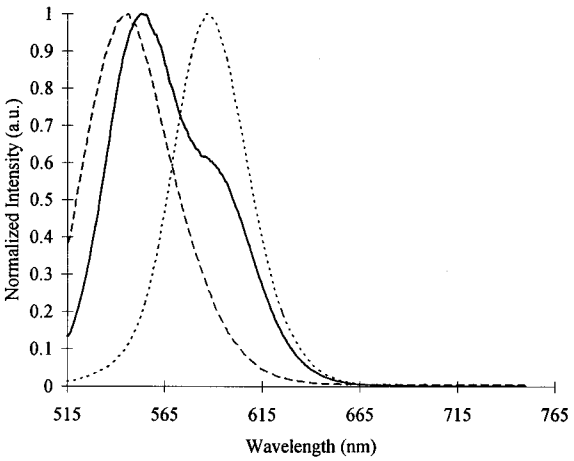

Figure 6. Fluorescence emission of Rhodamine-6G composite glass (dashed curve), ASPI composite glass (dotted curve), and the composite glass containing both dyes (solid curve).

Optical Characterization of the Composite Glasses. Figure 6 presents the fluorescence emission of the dye-doped composite glasses. The composite glass containing ASPI has an emission maximum at 586 nm, and the composite glass containing Rhodamine-6G has the emission maximum at 546 nm. The composite glass containing both dyes has emission from both with no significant quenching of emission from either dye. The peaks were reconstructed using a computer software program with an exponential Gaussian fit function. The peak of the ASPI emission is at 594 nm and that of Rhodamine-6G is at 552 nm. The fwhm of the emission for ASPI is 45 nm and that of Rhodamine-6G is 53 nm. In the glass containing both dyes the widths are respectively 41 nm for ASPI and 43 nm for Rhodamine-6G. The observed fluorescence emission (maxima and width) parameters in the composite glasses are presented in Table 1.

Lasing of the dye-doped composite glass was demonstrated in a cavity consisting of a ∼100% reflecting mirror and a ∼70%

(39) Eftink, M. R. Fluorescence Quenching: Theory and Application. *Topics in Fluorescence Spectroscopy*; Lakowicz, J. R., Ed.; Vol. 2, Plenum Press: New York, 1991; Vol. 2, Chapter 2.

(40) Ingle, J. D., Jr.; Crouch, S. R. *Spectrochemical Analysis*; Prentice Hall: Englewood Cliffs, NJ, 1988; p 343.

(41) Vogel, M.; Retting, W.; Sens, R.; Drexhage, K. H. *Chem. Phys. Lett.* **1988**, *147*, 452.

(42) Cheung, H. C. Resonance Energy Transfer. *Topics in Fluorescence Spectroscopy*; Lakowicz, J. R., Ed.; Plenum Press: New York, 1991; Vol. 2, Chapter 3.

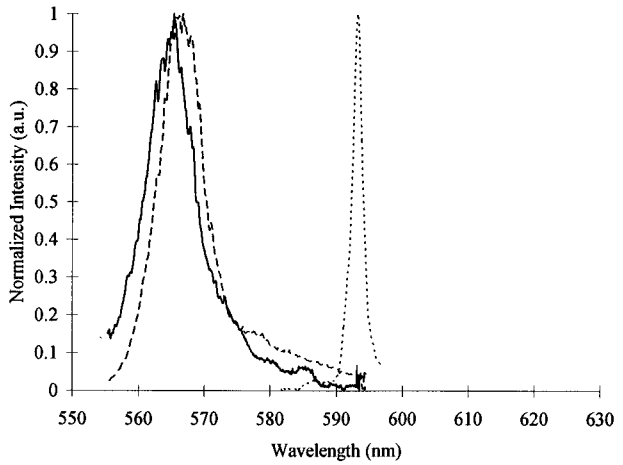

Figure 7. Lasing output intensity vs wavelength curves for Rhodamine-6G composite glass (solid curve), ASPI composite glass (dotted curve), and the composite glass containing both dyes (dashed curve). The composite glasses were transverse pumped with a 8 ns pulsed frequency-doubled Nd:YAG laser at 532 nm operating at a 1 Hz repetition rate, using a ∼100% reflecting mirror as the back reflector.

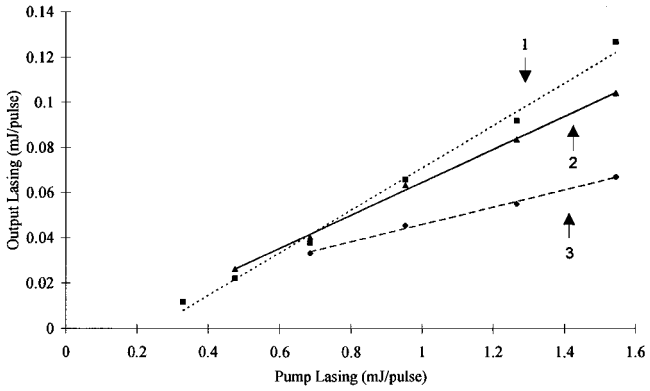

Figure 8. Lasing slope efficiency of composite glasses. Line 1 represents the ASPI composite glass, line 3 represents the Rhodamine-6G composite glass, and line 2 represents the composite glass containing both dyes. The least-squares best-fit line is drawn through the data points.

reflecting outcoupler. The wavelength dependence of the composite glass dye laser outputs are presented in Figure 7. The composite glass containing ASPI has a lasing emission maximum at ∼593 nm with a fwhm of 2 nm. The composite glass containing Rhodamine-6G has a lasing emission maximum at ∼565 nm with a fwhm of 5 nm. The composite glass containing both Rhodamine-6G and ASPI has a lasing emission maximum at ∼567 nm with a fwhm of 5 nm. It is not surprising that the preferable wavelength lasing mode in the multiphasic composite glass, in this cavity arrangement, is similar to that for pure Rhodamine-6G due to the better lasing characteristics of Rhodamine-6G and the cavity configuration itself.

Figure 8 is the lasing slope efficiency of the three composite glasses. The lasing slope efficiencies are as follows: ∼9% for the ASPI composite glass, ∼3% for the Rhodamine-6G composite glass, and ∼7% for the multiphasic composite glass containing both dyes. The observed data for the dye-doped composite glasses are summarized in Table 1. We feel that the relatively low efficiency of the Rhodamine-6G glass is mainly due to dimer or higher order aggregates that have formed in the glass. The doping level used was the highest possible, using Triton X-100 to increase the solubility and minimize aggregation. In general, lower efficiencies are observed in composite glass due to slight inhomogeneities compared to solution.

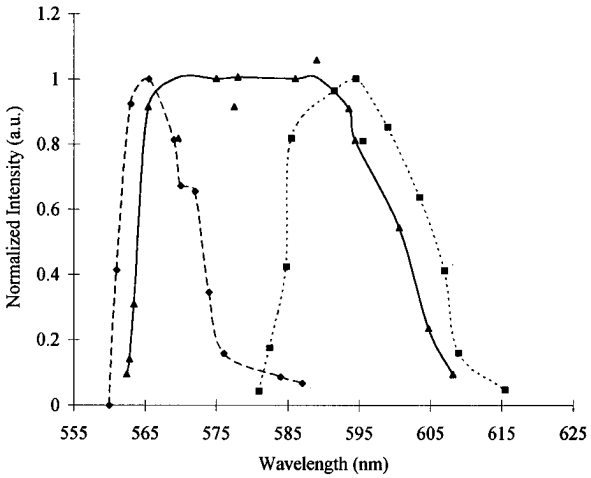

Figure 9. Lasing tunability of Rhodamine-6G composite glass (diamonds), ASPI composite glass (squares), and the multiphasic composite glass containing both Rhodamine-6G and ASPI (triangles). The composite glasses were transverse pumped with a 8 ns pulsed frequency-doubled Nd:YAG laser at 532 nm operating at a 1 Hz repetition rate, using a grating as the back reflector.

Figure 9 is the lasing tunability of the composite glasses. Tunable narrow band laser outputs were observed in a cavity consisting of a grating as the back reflector and a ∼70% reflecting outcoupler. The fwhm of the tunability spectra for the ASPI composite glass is ∼21 nm and that for Rhodamine-6G ∼12 nm. For the composite glass containing both dyes it is ∼37 nm. From these data it is evident that the glass containing both dyes is tunable across the range of both dyes (560−610 nm), where as in the solution state Rhodamine-6G emission is quenched. The narrowing of the tunability in the composite glasses compared to solution is also a result of the less homogeneous nature of the matrix compared to solution; however, we feel that this feature can be significantly improved under more carefully controlled preparation conditions. The tunability ranges are presented in Table 1 as well. This result represents the fascinating possibilities embodied in the multiphasic composite glasses for fabricating multifunctional devices for photonics, in this case a multi-dyed solid state laser tunable over a wide wavelength range.

As was previously mentioned we believe that the quenching in the solution state is a result of Förster energy transfer. A detailed discussion of the Förster energy transfer process follows. We consider the shape of the pores to be cylindrical, since our porous glass is obeying the equation for the relation between the diameter and the specific surface area for the cylindrical case as reported by Yamane.[43] When calculating the distance between the adsorbed molecules on the pore surface and the molecules in the pores of the multiphasic composite glass we must consider the ratio between the specific surface area and the pore volume. Therefore, reducing the problem to two dimensions only, we used the following equation:

$$d = \sqrt{\frac{1000}{CN_aP_v}S_a} \tag{4}$$

where d is the distance (in cm) between molecules deposited on the surface of the pores (in cm), C is the concentration (in mol/L) of the solution used to deposit the molecules, N_a is Avogadro's number, P_v is the pore volume per 1 cm^3, and S_a is

(43) Yamane, M. Monolith Formation from the Sol-Gel Process. *Sol-Gel Technology for Thin Films, Fibers, Preforms, Electronics and Specialty Shapes*; Klein, L. C., Ed.; Noyes Publications: Park Ridge, NJ, 1988; Chapter 10.

the surface area per 1 cm^3. This calculation reveals that, when compared to the same concentration in the solution state the distance between ASPI molecules is increased from 80 to 210 Å. This is due to the extremely large surface area to volume (of the pores) ratio which is $\sim 8.5 \times 10^6$. This implies that for the same concentration in the composite glass and in solution the distance between the molecules has increased in the composite glass. If we assume that Rhodamine-6G is in the center of the cylindrical pores, then the distance between the ASPI and Rhodamine-6G molecules is increased from 70 to 110 Å. This represents an increase in the distance between the ASPI and Rhodamine-6G molecules by a factor of 1.6.

The rate of energy transfer between the donor molecule (Rhodamine-6G) and the acceptor molecule (ASPI) in the Förster energy transfer mechanism can be described by the following equation:[42]

$$k_T = \frac{9(\ln 10)\kappa^2 Q_d J}{128\pi^5 n^4 N \tau_d R^6} \quad (5)$$

where κ^2 is the orientational factor for the dipole−dipole interaction, Q_d is the fluorescence quantum yield of the donor molecule without the acceptor molecule, n is the refractive index of the medium, N_a is Avogadro's number, τ_d is the fluorescence lifetime of the donor molecule without the presence of the acceptor, R is the distance between the centers of the donor and the acceptor molecules, and J is the normalized spectral overlap integral. From eq 5 the rate of energy transfer is directly proportional to the orientational factor κ to the second power and inversely proportional to the sixth power of the distance between the center of the molecules. It is these two factors that we believe are significantly changed in the multiphasic composite glass. By increasing the distance between the molecules by a factor of 1.6 we have decreased the rate of energy transfer by more than one order of magnitude. Also, in the solution state, the molecules are free to rotate and sample most if not all of the orientational possibilities during the excited state lifetime of Rhodamine-6G. In the solid state the molecules are effectively frozen in place with little or no rotation allowed leading to a further decrease in the energy transfer.[42] Due to the change in the distance between the molecules and the decrease of the orientational factor we have succeeded in preventing quenching due to Förster energy transfer (and other potential quenching mechanisms) in the multiphasic energy. We plan to pursue this type of study further to elucidate the unique properties of multiphasic nanostructured composite glasses relative to other materials in caging molecules in separate phases.

Conclusions

In this paper the preparation, optical characterization, and energy transfer in a multi-dye tunable solid state laser is presented. The lasing medium consists of a multiphasic nanostructured composite that has two dyes in two different phases of the material. The material is a sol-gel derived porous glass where the pores are filled with an organic polymer. A new laser dye, ASPI, is in the interfacial phase of the composite glass while Rhodamine-6G is in the polymer phase. The lasing performance of the solid state material is compared to that in the solution state. We demonstrate that in the multiphasic nanostructured composite both dyes are active as lasing media (with an efficiency of ~7%) and the glass is tunable across the tuning range of both dyes (560−610 nm). We also demonstrate that in solution, on the other hand, the emission from one of the dyes (Rhodamine-6G) is completely quenched. From this comparison we have been able to demonstrate the differences between the solution state and the composite glass state. The proposed mechanism of quenching is Förster energy transfer, which is effective in solution but not in the composite glass, due to significant increases in the distance between the two dyes as a result of the extremely high ratio of interfacial surface area to pore volume as well as due to a reduction of the orientational factor. We believe that this work is another demonstration of promising properties of multiphasic nanostructured composite glasses for fabricating multifunctional materials for photonics.

Furthermore, a new lasing dye (ASPI) has been characterized by linear spectroscopy and its lasing properties have been studied. The results of this characterization reveal a dye with a low fluorescence quantum yield ($\sim 7 \times 10^{-3}$) but high lasing efficiency (~13.5%) under pulsed pump conditions. From this we infer that there is an intersystem crossing occurring from the S_1 to the T_1 state in the dye; however, under pulsed nanosecond conditons the dye is stimulated to emit at a rate faster than the rate at which the T_1 state can be significantly populated. In addition, this chromophore has interesting properties such as two-photon absorption-induced lasing that have been reported else where.

Acknowledgment. The authors are indebted to Ms. Chan F. Zhao for synthesizing *trans*-4-[P-(*N*-ethyl-*N*-(hydroxyethyl)-amino)styryl]-*N*-(hydroxyethyl)pyridinium iodide (ASPI). The authors also thank Mr. Leonard A. Baker for his diligent help with the preparation of the composite glasses and solutions. The current work was sponsored by the Air Force Office of Scientific Research and the Polymer Branch of Wright Laboratory through Contract No. F49620-93-C0017.

JA952926Q